

Renormalized Quantum Stress-Energy Tensor of a Nonzero Radius Cosmic String

Noah Graham^{1,*}

¹*Department of Physics, Middlebury College, Middlebury, Vermont 05753, USA*

We calculate the effects of quantum fluctuations of a scalar field in the “ballpoint pen” cosmic string geometry. Using the approach to renormalization established previously for the energy density in two space dimensions, we extend those calculations to $3 + 1$ dimensions, nonzero scalar mass, and the full stress-energy tensor, including its contribution to the null energy condition for radial geodesics. The calculation demonstrates in detail the process of renormalization in curved spacetime, including the effects of the conformal anomaly. This calculation provides one of the few examples where quantum effects in curved spacetime can be explicitly calculated.

I. INTRODUCTION

Curved space backgrounds present unique challenges for renormalization in quantum field theory. In topologically nontrivial backgrounds, such calculations must compare fluctuations between globally distinct sectors, while consistently imposing precise renormalization conditions. In a $3 + 1$ dimensional model, one must go beyond renormalization of the Einstein-Hilbert term $\frac{\mathcal{R}}{8\pi G}$, written in terms of the Ricci scalar \mathcal{R} and gravitational constant G , to include higher-order counterterms proportional to \mathcal{R}^2 and $\square\mathcal{R}$ in the effective action. Although the effects of these terms are too small for their coefficients to be measured, they play an important role in fundamental features of quantum field theory in curved spacetime, including the conformal anomaly [1].

Cosmic string geometries [2–7] can provide a valuable theoretical laboratory in which to study these effects. With curvature only in the spatial r - θ plane perpendicular to the string axis, they provide a geometry in which it is tractable to compute the scattering data required to analyze quantum fluctuations. At the same time, they demonstrate topological effects through a deficit angle that persists at large distances. Such calculations were first carried out in the “point string” model, where one approximates the string to have infinitesimal thickness, with a corresponding divergence in the curvature yielding a finite, nonzero integral over the string cross section [2–4]. To remove this unphysical idealization, the curvature can be spread over nonzero thickness by introducing a string radius r_0 . In the “flowerpot” model, the curvature is localized to a cylindrical surface at $r = r_0$, while the “ballpoint pen” model has constant nonzero curvature over a solid cylinder from $r = 0$ to $r = r_0$ [5–7]. While both can be treated by the methods described here, the ballpoint pen is of greater interest because it is both fully nonsingular and contains extended regions (rather than isolated singularities) at which the curvature is nonzero, giving contributions from renormalization counterterms.

This paper extends techniques previously applied to the quantum energy density of a massless scalar field in the background of a cosmic string in $2 + 1$ dimensions [8] to compute the full renormalized stress-energy tensor in a $3 + 1$ -dimensional model. In two space dimensions the geometry is conformally flat, and renormalization can be expressed entirely in terms of the $1 + 1$ -dimensional trace anomaly [9–11], which is linear in \mathcal{R} . Extending to $3 + 1$ dimensions then requires the introduction of quadratic counterterms. By first generalizing to a massive particle, this calculation shows how the conformal anomaly emerges from the second-order renormalization counterterm through a quantum contribution to the trace of the stress-energy tensor that persists even as the scalar mass goes to zero.

After introducing the field theory model in Sec. II and the associated scattering theory in Sec. III, in Sec. IV we establish the key calculational tools used here, which give the connection developed in Ref. [12] between quantum expectation values and analytic scattering data, as carried out in dimensional regularization for a background that is spherically symmetric in m dimensions and translationally invariant in n dimensions. In this process, the heat kernel coefficients used to define renormalization in curved spacetime then emerge from the leading terms in the Born approximation. To make the calculation numerically tractable, we add and subtract the result for the point string as an intermediate result in Sec. V, and illustrate particular subtleties of this process for the calculation of the difference between the radial and angular pressures in Sec. VI. We show numerical results in Sec. VII, and summarize the calculation in Sec. VIII.

*Electronic address: ngraham@middlebury.edu

II. MODEL AND GREEN'S FUNCTION

We consider a free scalar field of mass μ in 3 + 1 spacetime dimensions, for which the action functional is

$$S = -\frac{1}{2} \int d^d x \sqrt{-g} (\nabla_\alpha \phi \nabla^\alpha \phi + \xi \mathcal{R} \phi^2 + \mu^2 \phi^2), \quad (1)$$

including coupling ξ to the Ricci curvature scalar \mathcal{R} . Of particular interest is the case of conformal coupling, $\xi = \frac{1}{6}$. The equation of motion is

$$-\nabla_\alpha \nabla^\alpha \phi + \xi \mathcal{R} \phi + \mu^2 \phi = 0 \quad (2)$$

with metric signature $(-+++)$. The stress-energy tensor is given by [13–15]

$$T_{\alpha\beta} = \nabla_\alpha \phi \nabla_\beta \phi - g_{\alpha\beta} \frac{1}{2} (\nabla_\gamma \phi \nabla^\gamma \phi + \mu^2 \phi^2) + \xi \phi^2 \left(R_{\alpha\beta} - \frac{1}{2} g_{\alpha\beta} \mathcal{R} \right) + \xi (g_{\alpha\beta} \nabla_\gamma \nabla^\gamma - \nabla_\alpha \nabla_\beta) (\phi^2), \quad (3)$$

as obtained by varying the action with respect to the metric. Note that the curvature coupling contributes to the stress-energy tensor even in regions where $\mathcal{R} = 0$, although it does so by a total derivative.

We consider the spacetime metric [5–7]

$$ds^2 = -dt^2 + p(r)^2 dr^2 + r^2 d\theta^2 + dz^2 \quad (4)$$

with a deficit angle $2\theta_0$, meaning that the range of angular coordinate is $0 \dots 2(\pi - \theta_0)$, and we define $\sigma = \frac{\pi}{\pi - \theta_0}$. To implement the deficit angle without a singularity at the origin, we introduce a profile function $p(r)$ that ranges from $\frac{1}{\sigma}$ at the origin to 1 at the string radius r_0 . The nonzero Christoffel symbols in this geometry are

$$\Gamma_{rr}^r = \frac{p'(r)}{p(r)} \quad \Gamma_{\theta\theta}^r = -\frac{r}{p(r)^2} \quad \Gamma_{\theta r}^\theta = \Gamma_{r\theta}^\theta = \frac{1}{r}, \quad (5)$$

and because the geometry only has curvature in two dimensions, all the nonzero components of the Riemann and Ricci tensors

$$R_{\theta r\theta}^r = -R_{r\theta r}^\theta = R_{\theta\theta} = g_{\theta\theta} \frac{\mathcal{R}}{2} \quad R_{r\theta r}^\theta = -R_{r r\theta}^\theta = R_{rr} = g_{rr} \frac{\mathcal{R}}{2} \quad (6)$$

can be expressed in terms of the curvature scalar $\mathcal{R} = \frac{2}{r} \frac{p'(r)}{p(r)^3}$. It obeys the Gauss-Bonnet theorem in the r - θ plane,

$$\int_0^{r_0} p(r) dr \int_0^{2\pi/\sigma} r d\theta \mathcal{R} = \frac{4\pi}{\sigma} \int_0^{r_0} \frac{p'(r)}{p(r)^2} dr = \left(-\frac{4\pi}{\sigma} \frac{1}{p(r)} \right) \Big|_{r=0}^{r=r_0} = 4\pi \left(1 - \frac{1}{\sigma} \right) = 4\theta_0, \quad (7)$$

for any $p(r)$ obeying the boundary conditions given above.

Acting on any scalar χ , the covariant derivatives simply become ordinary derivatives, while for second derivatives we have nontrivial contributions from the Christoffel symbols given above,

$$\nabla_\theta \nabla_\theta \chi = \partial_\theta^2 \chi - \Gamma_{\theta\theta}^r \partial_r \chi \quad \nabla_r \nabla_r \chi = \partial_r^2 \chi - \Gamma_{rr}^r \partial_r \chi \quad \nabla_r \nabla_\theta \chi = \nabla_\theta \nabla_r \chi = \partial_\theta \partial_r \chi - \Gamma_{r\theta}^\theta \partial_\theta \chi, \quad (8)$$

and, as a result, covariant derivatives with respect to θ can be nonzero even if χ is rotationally invariant. In particular, we have

$$(g^{\theta\theta} \nabla_\theta \nabla_\theta + g^{rr} \nabla_r \nabla_r) \chi = \frac{1}{r^2} \left(\frac{\partial^2 \chi}{\partial \theta^2} + \mathcal{D}_r^2 \right) \chi, \quad (9)$$

where $\mathcal{D}_r = \frac{r}{p(r)} \frac{\partial}{\partial r}$ is the radial derivative. The equation of motion for ϕ then becomes

$$\left(\frac{\partial^2}{\partial t^2} - \frac{1}{r^2} \mathcal{D}_r^2 - \frac{1}{r^2} \frac{\partial^2}{\partial \theta^2} - \frac{d^2}{dz^2} + \mu^2 + \xi \mathcal{R} \right) \phi = 0, \quad (10)$$

which in combination with $\mathcal{D}_r^2(\phi^2) = 2(\mathcal{D}_r\phi)^2 + 2\phi\mathcal{D}_r^2\phi$ gives the relation between expectation values

$$\left\langle \frac{1}{4r^2}\mathcal{D}_r^2(\phi^2) \right\rangle = \left\langle \frac{1}{2r^2}(\mathcal{D}_r\phi)^2 - \frac{1}{2}(\partial_t\phi)^2 + \frac{1}{2r^2}(\partial_\theta\phi)^2 + \frac{1}{2}(\partial_z\phi)^2 + \frac{\mu^2}{2}\phi^2 + \frac{\xi}{2}\mathcal{R}\phi^2 \right\rangle - \mathcal{A}, \quad (11)$$

where \mathcal{A} is an anomalous contribution discussed below and we have used $\langle(\partial_t\phi)^2\rangle = -\langle\phi(\partial_t^2\phi)\rangle$, and similarly for the θ and z derivatives. We therefore obtain the stress-energy tensor

$$\begin{aligned} \langle T_t^t \rangle &= -\langle \mathcal{H} \rangle = -\left\langle \frac{1}{2}(\partial_t\phi)^2 + \frac{1}{2r^2}(\mathcal{D}_r\phi)^2 + \frac{1}{2r^2}(\partial_\theta\phi)^2 + \frac{1}{2}(\partial_z\phi)^2 + \frac{\mu^2}{2}\phi^2 + \frac{\xi}{2}\mathcal{R}\phi^2 - \frac{\xi}{r^2}\mathcal{D}_r^2(\phi^2) \right\rangle \\ &= -\left\langle (\partial_t\phi)^2 + \left(\frac{1}{4} - \xi\right) \frac{1}{r^2}\mathcal{D}_r^2(\phi^2) \right\rangle + \mathcal{A} \\ \langle T_r^r \rangle &= \left\langle \frac{1}{2}(\partial_t\phi)^2 + \frac{1}{2r^2}(\mathcal{D}_r\phi)^2 - \frac{1}{2r^2}(\partial_\theta\phi)^2 - \frac{1}{2}(\partial_z\phi)^2 - \frac{\mu^2}{2}\phi^2 + \frac{\xi}{r^2} \frac{1}{p(r)}\mathcal{D}_r(\phi^2) \right\rangle \\ &= \left\langle \frac{1}{r^2}(\mathcal{D}_r\phi)^2 - \frac{1}{4r^2}\mathcal{D}_r^2(\phi^2) + \frac{\xi}{r^2} \frac{1}{p(r)}\mathcal{D}_r(\phi^2) + \frac{\xi}{2}\mathcal{R}\phi^2 \right\rangle + \mathcal{A} \\ \langle T_\theta^\theta \rangle &= \left\langle \frac{1}{2}(\partial_t\phi)^2 - \frac{1}{2r^2}(\mathcal{D}_r\phi)^2 + \frac{1}{2r^2}(\partial_\theta\phi)^2 - \frac{1}{2}(\partial_z\phi)^2 - \frac{\mu^2}{2}\phi^2 + \frac{\xi}{r^2} \left(\mathcal{D}_r^2(\phi^2) - \frac{1}{p(r)}\mathcal{D}_r(\phi^2) \right) \right\rangle \\ &= \left\langle \frac{1}{r^2}(\partial_\theta\phi)^2 - \left(\frac{1}{4} - \xi\right) \frac{1}{r^2}\mathcal{D}_r^2(\phi^2) - \frac{\xi}{r^2} \frac{1}{p(r)}\mathcal{D}_r(\phi^2) + \frac{\xi}{2}\mathcal{R}\phi^2 \right\rangle + \mathcal{A} \\ \langle T_z^z \rangle &= \left\langle \frac{1}{2}(\partial_t\phi)^2 - \frac{1}{2r^2}(\mathcal{D}_r\phi)^2 - \frac{1}{2r^2}(\partial_\theta\phi)^2 + \frac{1}{2}(\partial_z\phi)^2 - \frac{\mu^2}{2}\phi^2 - \frac{\xi}{2}\mathcal{R}\phi^2 + \frac{\xi}{r^2}\mathcal{D}_r^2(\phi^2) \right\rangle \\ &= \left\langle (\partial_z\phi)^2 - \left(\frac{1}{4} - \xi\right) \frac{1}{r^2}\mathcal{D}_r^2(\phi^2) \right\rangle + \mathcal{A} \end{aligned} \quad (12)$$

where we have used mixed indices to simplify metric factors and $\langle \mathcal{H} \rangle$ denotes the energy density. By Lorentz symmetry in the z direction, we have $\langle(\partial_t\phi)^2\rangle = -\langle(\partial_z\phi)^2\rangle$ and $\langle T_t^t \rangle = \langle T_z^z \rangle$.

We define the Green's function $G_\sigma(\mathbf{r}, \mathbf{r}', \kappa, k_z)$ for imaginary wave number $k = i\kappa$ and transverse momentum k_z , which obeys

$$\left(-\frac{1}{r^2}\mathcal{D}_r^2 - \frac{1}{r^2}\frac{\partial^2}{\partial\theta^2} - \frac{\partial^2}{\partial z^2} + \xi\mathcal{R} + \mu^2\phi^2 + \kappa^2 + k_z^2 \right) G_\sigma(\mathbf{r}, \mathbf{r}', \kappa, k_z) = \frac{1}{rp(r)}\delta(r-r')\delta(\theta-\theta')e^{ik_z(z-z')}, \quad (13)$$

and we consider the ‘‘ballpoint pen’’ profile function

$$p(r) = \begin{cases} \left[\sigma^2 - \frac{r^2}{r_0^2}(\sigma^2 - 1) \right]^{-1/2} & r < r_0 \\ 1 & r > r_0 \end{cases}, \quad (14)$$

where r_0 is the string radius, which has constant curvature $\mathcal{R} = \frac{2(\sigma^2 - 1)}{r_0^2}$ inside and zero curvature outside. The ‘‘flowerpot’’ model, with zero curvature everywhere except for a δ -function contribution at the string radius, can also be calculated straightforwardly using the same techniques, but that case does not fully demonstrate the renormalization process because the curvature is zero for all $r \neq r_0$, and as a result after subtracting the free contribution the result is already finite, with all other counterterms vanishing.

III. SCATTERING WAVE FUNCTIONS

We write the Green's function in the scattering form

$$G_\sigma(\mathbf{r}, \mathbf{r}', \kappa, k_z) = \frac{\sigma}{\pi} \sum_{\ell=0}^{\infty} {}' \psi_{\kappa, k_z, \ell}^{\text{reg}}(r_<) \psi_{\kappa, k_z, \ell}^{\text{out}}(r_>) \cos[\sigma\ell(\theta - \theta')] e^{ik_z(z-z')}, \quad (15)$$

where the prime on the sum indicates that the $\ell = 0$ term is counted with a weight of one-half, arising because we have written the sum over nonnegative ℓ only. The radial wavefunctions obey the equation

$$\left[-\frac{1}{r^2}\mathcal{D}_r^2 + \frac{\ell^2\sigma^2}{r^2} + \xi\mathcal{R} + \mu^2\phi^2 + \kappa^2 + k_z^2 \right] \psi_{\kappa, k_z, \ell}(r) = 0, \quad (16)$$

where the regular solution is defined to be well-behaved at $r = 0$, while the outgoing solution obeys outgoing wave boundary conditions for $r \rightarrow \infty$, normalized to unit amplitude. Here $r_<$ ($r_>$) is the smaller (larger) axial radius of \mathbf{r} and \mathbf{r}' . The regular functions are normalized so that they obey the Wronskian relation

$$\frac{d}{dr} \left(\psi_{\kappa, k_z, \ell}^{\text{reg}}(r) \right) \psi_{\kappa, k_z, \ell}^{\text{out}}(r) - \psi_{\kappa, k_z, \ell}^{\text{reg}}(r) \frac{d}{dr} \left(\psi_{\kappa, k_z, \ell}^{\text{out}}(r) \right) = \frac{p(r)}{r}, \quad (17)$$

which provides the appropriate jump condition for the Green's function.

Next we construct the scattering wavefunctions in the string background. As shown in Ref. [7], we can write the full regular and outgoing solutions in terms of Legendre and Bessel functions as

		$r < r_0$	$r > r_0$
$\psi_{\kappa, k_z, \ell}(r) =$	regular	$A_{\kappa, k_z, \ell} P_{\nu(\kappa, k_z)}^{\ell} \left(\frac{1}{\sigma p(r)} \right)$	$I_{\sigma \ell}(\sqrt{\kappa^2 + k_z^2} r) + B_{\kappa, k_z, \ell} K_{\sigma \ell}(\sqrt{\kappa^2 + k_z^2} r)$
	outgoing	$C_{\kappa, k_z, \ell} P_{\nu(\kappa, k_z)}^{\ell} \left(\frac{1}{\sigma p(r)} \right) + D_{\kappa, k_z, \ell} Q_{\nu(\kappa, k_z)}^{\ell} \left(\frac{1}{\sigma p(r)} \right)$	$K_{\sigma \ell}(\sqrt{\kappa^2 + k_z^2} r)$

(18)

with

$$\nu(\kappa, k_z) = -\frac{1}{2} + \frac{1}{2} \sqrt{(1 - 8\xi) - \frac{4(\kappa^2 + k_z^2)r_0^2}{\sigma^2 - 1}}. \quad (19)$$

Matching boundary conditions at $r = r_0$, we obtain the following for the combinations of coefficients we will need in the calculation,

$$\begin{aligned} A_{\kappa, k_z, \ell} D_{\kappa, k_z, \ell} &= \frac{1}{\sigma} \frac{\Gamma(\nu(\kappa, k_z) - \ell + 1)}{\Gamma(\nu(\kappa, k_z) + \ell + 1)} \\ \frac{C_{\kappa, k_z, \ell}}{D_{\kappa, k_z, \ell}} &= -\frac{(\sigma^2 - 1) Q_{\nu(\kappa, k_z)}^{\ell} \left(\frac{1}{\sigma} \right) K_{\sigma \ell} \left(\sqrt{\kappa^2 + k_z^2} r_0 \right) + \sigma \kappa r_0 Q_{\nu(\kappa, k_z)}^{\ell} \left(\frac{1}{\sigma} \right) K'_{\sigma \ell} \left(\sqrt{\kappa^2 + k_z^2} r_0 \right)}{(\sigma^2 - 1) P_{\nu(\kappa, k_z)}^{\ell} \left(\frac{1}{\sigma} \right) K_{\sigma \ell} \left(\sqrt{\kappa^2 + k_z^2} r_0 \right) + \sigma \kappa r_0 P_{\nu(\kappa, k_z)}^{\ell} \left(\frac{1}{\sigma} \right) K'_{\sigma \ell} \left(\sqrt{\kappa^2 + k_z^2} r_0 \right)} \\ B_{\kappa, k_z, \ell} &= -\frac{(\sigma^2 - 1) P_{\nu(\kappa, k_z)}^{\ell} \left(\frac{1}{\sigma} \right) I_{\sigma \ell} \left(\sqrt{\kappa^2 + k_z^2} r_0 \right) + \sigma \kappa r_0 P_{\nu(\kappa, k_z)}^{\ell} \left(\frac{1}{\sigma} \right) I'_{\sigma \ell} \left(\sqrt{\kappa^2 + k_z^2} r_0 \right)}{(\sigma^2 - 1) P_{\nu(\kappa, k_z)}^{\ell} \left(\frac{1}{\sigma} \right) K_{\sigma \ell} \left(\sqrt{\kappa^2 + k_z^2} r_0 \right) + \sigma \kappa r_0 P_{\nu(\kappa, k_z)}^{\ell} \left(\frac{1}{\sigma} \right) K'_{\sigma \ell} \left(\sqrt{\kappa^2 + k_z^2} r_0 \right)}, \end{aligned} \quad (20)$$

where prime denotes a derivative with respect to the function's argument.

As shown in Refs. [8, 16, 17], for $r < r_0$ the wave equation in the string background for angular momentum channel ℓ can be rewritten in terms of the rescaled field $\phi_{\kappa, k_z, \ell}(r_*) = \sqrt{r} \psi_{\kappa, k_z, \ell}(r)$ and the physical distance variable $r_* = \frac{r_0}{\sqrt{\sigma^2 - 1}} \arccos \frac{1}{\sigma p(r)}$ as

$$\left[-\frac{d^2}{dr_*^2} + \left(\frac{\ell^2 - \frac{1}{4}}{r_*^2} \right) + V_{\ell}(r) + \kappa^2 + k_z^2 \right] \phi_{\kappa, k_z, \ell}(r_*) = 0, \quad (21)$$

where the potential is

$$V_{\ell}(r) = \frac{(\ell^2 - \frac{1}{4}) \sigma^2}{r^2} - \frac{(\ell^2 - \frac{1}{4}) (\sigma^2 - 1)}{r_0^2 \left(\arccos \frac{1}{\sigma p(r)} \right)^2} + \frac{(8\xi - 1) (\sigma^2 - 1)}{4r_0^2}. \quad (22)$$

For use in the renormalization calculation below, we note that this potential can be expanded in the curvature,

$$V_{\ell}(r) = \frac{(\ell^2 - 1 + 6\xi)(\sigma^2 - 1)}{3r_0^2} + \frac{r^2(\ell^2 - \frac{1}{4})(\sigma^2 - 1)^2}{15r_0^4} + \mathcal{O} \left[\left(\frac{\sigma^2 - 1}{r_0^2} \right)^3 \right]. \quad (23)$$

We will make use of this expansion to determine renormalization counterterms that emerge from analysis of the corresponding scattering data.

IV. RENORMALIZED EXPECTATION VALUES AND ANOMALY

We begin by computing expectation values that make up the energy density, using results from Refs. [8, 12], adapted here to the case of a configuration that is symmetric in $m = 2$ dimensions and constant in $n = 1$ dimension.

For $z = z'$, the Green's function can be simplified to $G_\sigma(\mathbf{r}, \mathbf{r}', \bar{\kappa}) = G_\sigma(\mathbf{r}, \mathbf{r}', \kappa, k_z)$, where $\bar{\kappa} = \sqrt{\kappa^2 + k_z^2}$, with the corresponding wavefunctions denoted as $\psi_{\bar{\kappa}, \ell}(r) = \psi_{\kappa, k_z, \ell}(r)$. The expectation values can then be expressed in terms of this Green's function at coincident points as

$$\langle (\partial_t \phi)^2 \rangle = -\frac{1}{4\pi} \int_\mu^\infty \bar{\kappa}(\bar{\kappa}^2 - \mu^2) d\bar{\kappa} \left[G_\sigma(r, r, \bar{\kappa}) - G^{\text{free}}(r, r, \bar{\kappa}) + \frac{\mathcal{R}}{4\pi\bar{\kappa}^2} \left(\xi - \frac{1}{6} \right) - \frac{\mathcal{R}^2}{120\pi\bar{\kappa}^2} (1 - 10\xi + 30\xi^2) f(\bar{\kappa}, M) \right], \quad (24)$$

where the last three terms represent free space, linear, and quadratic counterterms, respectively. As shown in Ref. [8], the counterterm linear in \mathcal{R} arises as the limit of the divergence as $m \rightarrow 2$ of the free Green's function at $r \rightarrow 0$ times an explicit factor of $m - 2$, all of which multiplies the first-order term in Eq. (23) for $\ell = 0$. Because both the second-order contribution to the potential and the first-order wavefunctions vanish at $r = 0$, no such subtlety arises at second order, and the counterterm is simply given in terms of the second-order heat kernel coefficient [1], which for our configuration with constant curvature becomes

$$\frac{1}{180} R_{\alpha\beta\gamma\delta} R^{\alpha\beta\gamma\delta} - \frac{1}{180} R_{\alpha\beta} R^{\alpha\beta} + \frac{1}{2} \left(\frac{1}{6} - \xi \right)^2 \mathcal{R}^2 + \frac{1}{6} \left(\frac{1}{5} - \xi \right) \square \mathcal{R} = \frac{\mathcal{R}^2}{60} (1 - 10\xi + 30\xi^2). \quad (25)$$

It is multiplied by the kinematic function arising from second-order perturbation theory [12]

$$f(\bar{\kappa}, M) = \frac{1}{4\bar{\kappa}^2 - M^2} \left(1 + \frac{4\bar{\kappa}^2 \arctan \frac{M}{\sqrt{4\bar{\kappa}^2 - M^2}}}{M\sqrt{4\bar{\kappa}^2 - M^2}} \right), \quad (26)$$

which is written in terms of the renormalization scale M . To avoid infrared singularities, this scale is typically set equal to the threshold 2μ , or to an imaginary value appropriate to a relevant scale of the system if $\mu = 0$.

Again using the results of Refs. [8, 12], we obtain for the second derivative term

$$\left\langle \frac{1}{r^2} \mathcal{D}_r^2(\phi^2) \right\rangle = \frac{1}{2\pi} \int_\mu^\infty d\bar{\kappa} \bar{\kappa} \left(\frac{1}{r^2} \mathcal{D}_r^2 G_\sigma(r, r, \bar{\kappa}) - \frac{1}{r^2} \mathcal{D}_r^2 G^{\text{free}}(r, r, \bar{\kappa}) - \frac{1}{4\pi} \mathcal{R} \right), \quad (27)$$

using the first-order counterterm obtained in Ref. [8] for the $2 + 1$ dimensional case. In that case, the geometry is conformally flat and the combined counterterm for the energy density from Eqs. (24) and (27) is given by the $1 + 1$ dimensional anomaly contribution $\frac{\mathcal{R}}{48\pi}$ [9–11]. The $3 + 1$ dimensional string is not conformally flat, and correspondingly Eq. (27) has an additional factor of 2 relative to Eq. (24), leading to a more complex expression for the first-order counterterm. In general we would also need a wavefunction renormalization counterterm as well, proportional to the second derivative of the curvature, but in our case this counterterm vanishes because the curvature is constant. Note that the derivative of the free Green's function at coincident points vanishes, since it depends only on the difference of its arguments, but we will find it convenient to include this term for subsequent manipulations.

Finally, if the field has nonzero mass, we will also need to compute

$$\langle \phi^2 \rangle = \frac{1}{2\pi} \int_\mu^\infty d\bar{\kappa} \bar{\kappa} (G_\sigma(r, r, \bar{\kappa}) - G^{\text{free}}(r, r, \bar{\kappa})). \quad (28)$$

These expectation values are the ingredients we will need to compute $\langle T_t^t \rangle = \langle T_z^z \rangle$, along with the sum of pressures

$$\begin{aligned} \langle T_r^r + T_\theta^\theta \rangle &= \left\langle \frac{1}{r^2} (\mathcal{D}_r \phi)^2 + \frac{1}{r^2} (\partial_\theta \phi)^2 - \left(\frac{1}{2} - \xi \right) \frac{1}{r^2} \mathcal{D}_r^2(\phi^2) + \xi R \phi^2 \right\rangle \\ &= \left\langle (\partial_t \phi)^2 - (\partial_z \phi)^2 + \frac{\xi}{r^2} \mathcal{D}_r^2(\phi^2) - \mu^2 \phi^2 \right\rangle + 2\mathcal{A} = \left\langle 2(\partial_t \phi)^2 + \frac{\xi}{r^2} \mathcal{D}_r^2(\phi^2) - \mu^2 \phi^2 \right\rangle + 2\mathcal{A}. \end{aligned} \quad (29)$$

Next we turn to the anomalous contribution \mathcal{A} in Eq. (11). It arises because while the operator expectation values formally agree, the right-hand side depends on the renormalization scale through the second-order counterterm contained within the expectation values $\langle (\partial_t \phi)^2 \rangle$ and $\langle (\partial_z \phi)^2 \rangle$, while the left-hand side has no such dependence. If we set the renormalization scale to be 2μ and integrate up to a cutoff Λ , this contribution becomes

$$\mathcal{A}_0 = \frac{1}{8\pi} \int_\mu^\Lambda d\bar{\kappa} \frac{\mathcal{R}^2}{120\pi\bar{\kappa}^2} (1 - 10\xi + 30\xi^2) \bar{\kappa}(\bar{\kappa}^2 - \mu^2) f(\bar{\kappa}, 2\mu)$$

$$\begin{aligned}
&= \frac{\mathcal{R}^2}{3840\pi^2}(1 - 10\xi + 30\xi^2) \int_{\mu}^{\Lambda} \frac{d\bar{\kappa}}{\bar{\kappa}} \left(1 + \frac{\bar{\kappa}^2 \arctan \frac{\mu}{\sqrt{\bar{\kappa}^2 - \mu^2}}}{\mu \sqrt{\bar{\kappa}^2 - \mu^2}} \right) \\
&= \frac{\mathcal{R}^2}{3840\pi^2}(1 - 10\xi + 30\xi^2) \left[\frac{\sqrt{\Lambda^2 - \mu^2}}{\mu} \arctan \frac{\mu}{\Lambda^2 - \mu^2} + \log \left(\frac{\Lambda}{\mu} \right)^2 \right]. \tag{30}
\end{aligned}$$

We can recognize the second term in brackets as the logarithmic divergence being subtracted by renormalization. In the limit $\Lambda \gg \mu$, the first term in brackets goes to 1, leaving the finite contribution

$$\mathcal{A} = \frac{\mathcal{R}^2}{3840\pi^2}(1 - 10\xi + 30\xi^2). \tag{31}$$

A similar anomalous contribution arises for solitons in 1 + 1 dimensional flat spacetime [18], where the full calculation can be carried out analytically in dimensional regularization.

For conformal coupling $\xi = \frac{1}{6}$ and $\mu = 0$, the trace of the stress-energy tensor $\langle T_{\alpha}^{\alpha} \rangle$ becomes equal to $4\mathcal{A}$. We therefore obtain the correct anomaly

$$\langle T_{\alpha}^{\alpha} \rangle = \frac{1}{2880\pi^2} (R_{\alpha\beta\gamma\delta} R^{\alpha\beta\gamma\delta} - R_{\alpha\beta} R^{\alpha\beta} - \square \mathcal{R}) = \frac{\mathcal{R}^2}{5760\pi^2} = 4\mathcal{A} \tag{32}$$

in that case. Note that if the curvature within the string were not constant, the additional counterterm needed in the derivative term would provide the $\square \mathcal{R}$ contribution to the anomaly.

V. CALCULATION USING POINT STRING

While formally correct, the expressions given so far are not yet in a suitable form for actual calculations, because the mismatch between the angular momentum quantum numbers $\sigma\ell$ and ℓ in the full and free Green's functions respectively prevents us from taking the difference of the sums term by term. To avoid this problem, we add and subtract the contribution of a zero radius ‘‘point string,’’ chosen so that its angular momentum matches the full Green's function. The mismatched quantum numbers are then contained in the difference between the point string Green's function and the free Green's function, which can be efficiently computed via analytic continuation in ℓ [8].

The scattering solutions for the point string can be obtained using the same techniques as for a conducting wedge [19, 20], but with periodic rather than perfectly reflecting boundary conditions. The resulting normalized scattering functions for the point string are $\psi_{\bar{\kappa},\ell}^{\text{reg,point}}(r) = I_{\sigma\ell}(\bar{\kappa}r)$ and $\psi_{\bar{\kappa},\ell}^{\text{out,point}}(r) = K_{\sigma\ell}(\bar{\kappa}r)$, and the Green's function becomes [2–4]

$$G_{\sigma}^{\text{point}}(\mathbf{r}, \mathbf{r}', \bar{\kappa}) = \frac{\sigma}{\pi} \sum_{\ell=0}^{\infty} 'I_{\sigma\ell}(\bar{\kappa}r_{<}) K_{\sigma\ell}(\bar{\kappa}r_{>}) \cos[\ell\sigma(\theta - \theta')]. \tag{33}$$

Setting $\sigma = 1$, we obtain the free Green's function

$$G^{\text{free}}(\mathbf{r}, \mathbf{r}', \bar{\kappa}) = \frac{1}{\pi} \sum_{\ell=0}^{\infty} 'I_{\ell}(\bar{\kappa}r_{<}) K_{\ell}(\bar{\kappa}r_{>}) \cos[\ell(\theta - \theta')] = \frac{1}{2\pi} K_0 \left(\bar{\kappa} \left| r e^{i\theta} - r' e^{i\theta'} \right| \right). \tag{34}$$

To calculate the difference between these expressions in the limit where the points coincide, we can rewrite the ℓ sum as a contour integral [8]

$$\Delta G_{\sigma}^{\text{point}}(r, r, \bar{\kappa}) = G_{\sigma}^{\text{point}}(r, r, \bar{\kappa}) - G^{\text{free}}(r, r, \bar{\kappa}) = \frac{1}{\pi^2} \int_0^{\infty} d\lambda K_{i\lambda}(\bar{\kappa}r) K_{i\lambda}(\bar{\kappa}r) \frac{\sinh \left[\frac{\lambda}{\sigma} \pi (\sigma - 1) \right]}{\sinh \frac{\lambda}{\sigma} \pi}, \tag{35}$$

yielding an expression that is well-behaved computationally. We note that for a massless scalar in three space dimensions, the complete calculation of the stress-energy tensor for the point string can be carried out exactly, giving [2–4]

$$\langle T_{\alpha}^{\beta} \rangle^{\text{point}, \mu=0} = \frac{1}{1440\pi^2 r^4} \left[(\sigma^4 - 1) \text{diag}(1, 1, -3, 1) + 20(6\xi - 1)(\sigma^2 - 1) \text{diag} \left(1, -\frac{1}{2}, \frac{3}{2}, 1 \right) \right] \tag{36}$$

for $\mu = 0$, with coordinates listed in the order t, r, θ, z .

In subtracting and adding back the point string contribution, we can choose the values of both σ and r that we use for the point string. While the result of the calculation is independent of this choice, since we add and subtract the same quantity, it is advantageous to choose values for which the subtraction is most effective at improving the numerical convergence. There are additional subtleties that arise for the difference of the radial and angular pressures, which we discuss below.

For all of these calculations, in calculating at radius r in the ballpoint pen background we will choose $\tilde{\sigma} = p(r)\sigma$ and $\tilde{r} = p(r)r$ for the point string. Note that this radius differs slightly from the physical radius r_* used in Ref. [8], which is the integral of $p(r)$ with respect to r rather than its product with r . The present choice avoids the need to subtract the additional logarithmic correction $\frac{1}{2\pi} \log \frac{r_*}{rp(r)}$ discussed there, which becomes particularly advantageous for the pressure difference calculation below. Throughout the calculation, we therefore replace

$$G_\sigma(r, r, \bar{\kappa}) - G^{\text{free}}(r, r, \bar{\kappa}) = G_\sigma(r, r, \bar{\kappa}) - G_\sigma^{\text{point}}(\tilde{r}, \tilde{r}, \bar{\kappa}) + \Delta G_\sigma^{\text{point}}(\tilde{r}, \tilde{r}, \bar{\kappa}) \quad (37)$$

and then carry out the subtraction term by term in the Green's function sum, while using Eq. (35) to compute the last term in Eq. (37). For the difference of the first two terms we have [8]

$$G_\sigma(r, r, \bar{\kappa}) - G_\sigma^{\text{point}}(\tilde{r}, \tilde{r}, \bar{\kappa}) = \frac{1}{\pi} \sum_{\ell=0}^{\infty} \left[\frac{\Gamma(\nu(\bar{\kappa}) - \ell + 1)}{\Gamma(\nu(\bar{\kappa}) + \ell + 1)} P_{\nu(\bar{\kappa})}^\ell \left(\frac{1}{\sigma p(r)} \right) \left(\frac{C_{\bar{\kappa}, \ell}}{D_{\bar{\kappa}, \ell}} P_{\nu(\bar{\kappa})}^\ell \left(\frac{1}{\sigma p(r)} \right) + Q_{\nu(\bar{\kappa})}^\ell \left(\frac{1}{\sigma p(r)} \right) \right) - \tilde{\sigma} I_{\tilde{\sigma} \ell}(\bar{\kappa} \tilde{r}) K_{\tilde{\sigma} \ell}(\bar{\kappa} \tilde{r}) \right] \quad (38)$$

for $r < r_0$ and

$$G_\sigma(r, r, \bar{\kappa}) - G_\sigma^{\text{point}}(r, r, \bar{\kappa}) = \frac{\sigma}{\pi} \sum_{\ell=0}^{\infty} B_{\bar{\kappa}, \ell} K_{\sigma \ell}(\bar{\kappa} r) K_{\sigma \ell}(\bar{\kappa} r) \quad (39)$$

for $r > r_0$, where both expressions are in the limit of coincident points.

When working with the derivative of this expression as in Eq. (27), we make the replacement

$$\frac{1}{r^2} \mathcal{D}_r^2 G_\sigma(r, r, \bar{\kappa}) - \frac{1}{r^2} \mathcal{D}_r^2 G^{\text{free}}(r, r, \bar{\kappa}) = \frac{1}{r^2} \mathcal{D}_r^2 G_\sigma(r, r, \bar{\kappa}) - \frac{1}{r^2} \bar{\mathcal{D}}_r^2 G_\sigma^{\text{point}}(\tilde{r}, \tilde{r}, \bar{\kappa}) + \frac{1}{r^2} \bar{\mathcal{D}}_r^2 \Delta G_\sigma^{\text{point}}(\tilde{r}, \tilde{r}, \bar{\kappa}) \quad (40)$$

where $\bar{\mathcal{D}}_r = r \frac{d}{dr}$ is the radial derivative for the point string. (When acting on the free Green's function, $\bar{\mathcal{D}}_r$ and \mathcal{D}_r are equivalent because this derivative is zero.) Here we have denoted $\bar{\mathcal{D}}_r^2 G_\sigma^{\text{point}}(\tilde{r}, \tilde{r}, \bar{\kappa}) = \bar{\mathcal{D}}_r^2 G_\sigma^{\text{point}}(r, r, \bar{\kappa})|_{r=\tilde{r}}$, and similarly for other derivatives at \tilde{r} . To compute the derivatives of the Green's function, we then use that for any pair of solutions $\psi^A(r)$ and $\psi^B(r)$ obeying Eq. (16), we have

$$\frac{1}{2r^2} \mathcal{D}_r^2 (\psi_{\bar{\kappa}, \ell}^A(r) \psi_{\bar{\kappa}, \ell}^B(r)) = \left(\frac{(\sigma \ell)^2}{r^2} + \xi \mathcal{R} + \mu^2 + \bar{\kappa}^2 \right) \psi_{\bar{\kappa}, \ell}^A(r) \psi_{\bar{\kappa}, \ell}^B(r) + \frac{1}{r^2} (\mathcal{D}_r \psi_{\bar{\kappa}, \ell}^A(r)) (\mathcal{D}_r \psi_{\bar{\kappa}, \ell}^B(r)) , \quad (41)$$

and by using recurrence relations we can simplify

$$\mathcal{D}_r Z_{\nu(\bar{\kappa})}^\ell = \frac{r \sqrt{\sigma^2 - 1}}{r_0} Z_{\nu(\bar{\kappa})}^{\ell+1} \left(\frac{1}{\sigma p(r)} \right) + \frac{\ell}{p(r)} Z_{\nu(\bar{\kappa})}^\ell \left(\frac{1}{\sigma p(r)} \right) , \quad (42)$$

where Z is either P or Q , and similarly for derivatives of Bessel functions as well.

We thus obtain the expectation values

$$\begin{aligned} \langle (\partial_t \phi)^2 \rangle &= -\frac{1}{4\pi} \int_\mu^\infty \bar{\kappa} (\bar{\kappa}^2 - \mu^2) d\bar{\kappa} \left[G_\sigma(r, r, \bar{\kappa}) - G_\sigma^{\text{point}}(\tilde{r}, \tilde{r}, \bar{\kappa}) + \Delta G_\sigma^{\text{point}}(\tilde{r}, \tilde{r}, \bar{\kappa}) \right. \\ &\quad \left. + \frac{\mathcal{R}}{4\pi \bar{\kappa}^2} \left(\xi - \frac{1}{6} \right) - \frac{\mathcal{R}^2}{120\pi \bar{\kappa}^2} (1 - 10\xi + 30\xi^2) f(\bar{\kappa}, M) \right] \\ \left\langle \frac{1}{r^2} \mathcal{D}_r^2 (\phi^2) \right\rangle &= \frac{1}{2\pi} \int_\mu^\infty d\bar{\kappa} \bar{\kappa} \left(\frac{1}{r^2} \mathcal{D}_r^2 G_\sigma(r, r, \bar{\kappa}) - \frac{1}{r^2} \bar{\mathcal{D}}_r^2 G_\sigma^{\text{point}}(\tilde{r}, \tilde{r}, \bar{\kappa}) + \frac{1}{r^2} \bar{\mathcal{D}}_r^2 \Delta G_\sigma^{\text{point}}(\tilde{r}, \tilde{r}, \bar{\kappa}) - \frac{1}{4\pi} \mathcal{R} \right) \end{aligned}$$

$$\langle \phi^2 \rangle = \frac{1}{2\pi} \int_{\mu}^{\infty} d\bar{\kappa} \bar{\kappa} \left(G_{\sigma}(r, r, \bar{\kappa}) - G_{\bar{\sigma}}^{\text{point}}(\tilde{r}, \tilde{r}, \bar{\kappa}) + \Delta G_{\bar{\sigma}}^{\text{point}}(\tilde{r}, \tilde{r}, \bar{\kappa}) \right). \quad (43)$$

As described above, in all of these expressions the difference of Green's functions $G_{\sigma}(r, r, \bar{\kappa}) - G_{\bar{\sigma}}^{\text{point}}(\tilde{r}, \tilde{r}, \bar{\kappa})$ can be taken term by term in the sum, while the $\Delta G_{\bar{\sigma}}^{\text{point}}(\tilde{r}, \tilde{r}, \bar{\kappa})$ contribution is finite on its own, and is given by Eq. (36) for the case of $\mu = 0$.

VI. PRESSURE DIFFERENCE

The last remaining quantity to compute is the pressure difference

$$\langle T_r^r - T_{\theta}^{\theta} \rangle = \left\langle \frac{1}{r^2} (\mathcal{D}_r \phi)^2 - \frac{1}{r^2} (\partial_{\theta} \phi)^2 - \frac{\xi}{r^2} \mathcal{D}_r^2(\phi^2) + \frac{2\xi}{r^2} \frac{1}{p(r)} \mathcal{D}_r(\phi^2) \right\rangle = -r \partial_r \langle T_r^r \rangle, \quad (44)$$

where the second relation represents the only nontrivial component of the conservation equation for the stress-energy tensor, and follows from the equation of motion, Eq. (10). The calculation of this quantity proceeds similarly to those above, but involves additional subtleties: First, this calculation is much more sensitive to the choice of $\bar{\sigma}$ and \tilde{r} values for the point string. As a result, to obtain a tractable calculation we must use precisely the values chosen above, while in the previous calculations this choice was merely a matter of numerical optimization. We also find that we need a scaling correction, similar to the logarithmic term described above, that depends sensitively on this choice.

The expectation value $\langle \mathcal{D}_r^2(\phi^2) \rangle$ has already been computed above, and the expectation value $\langle \mathcal{D}_r(\phi^2) \rangle$ is fully renormalized by subtracting the free contribution, which is again implemented via adding and subtracting the point string contribution,

$$\left\langle \frac{2\xi}{r^2} \frac{1}{p(r)} \mathcal{D}_r(\phi^2) \right\rangle = \frac{2\xi}{r^2} \frac{1}{p(r)} \cdot \frac{1}{2\pi} \int_{\mu}^{\infty} d\bar{\kappa} \bar{\kappa} \left(\mathcal{D}_r G_{\sigma}(r, r, \bar{\kappa}) - \bar{\mathcal{D}}_r G_{\bar{\sigma}}^{\text{point}}(\tilde{r}, \tilde{r}, \bar{\kappa}) + \bar{\mathcal{D}}_r \Delta G_{\bar{\sigma}}^{\text{point}}(\tilde{r}, \tilde{r}, \bar{\kappa}) \right), \quad (45)$$

where the derivative of the Green's function at coincident points yields a product rule for the two wavefunctions, $\mathcal{D}_r [\psi_{\bar{\kappa}, \ell}^A(r) \psi_{\bar{\kappa}, \ell}^B(r)] = [\mathcal{D}_r \psi_{\bar{\kappa}, \ell}^A(r)] \psi_{\bar{\kappa}, \ell}^B(r) + \psi_{\bar{\kappa}, \ell}^A(r) [\mathcal{D}_r \psi_{\bar{\kappa}, \ell}^B(r)]$. As a result, the only other expectation value we need to compute is, for $r < r_0$,

$$\begin{aligned} \left\langle \frac{1}{r^2} (\mathcal{D}_r \phi)^2 - \frac{1}{r^2} (\partial_{\theta} \phi)^2 \right\rangle &= \frac{1}{2\pi r^2} \int_{\mu}^{\infty} d\bar{\kappa} \bar{\kappa} \left(\frac{1}{\pi} \sum_{\ell=0}^{\infty} \left\{ [\mathcal{D}_r P_{\nu(\bar{\kappa})}^{\ell} \left(\frac{1}{\sigma p(r)} \right)] [\mathcal{D}_r R_{\nu(\bar{\kappa})}^{\ell} \left(\frac{1}{\sigma p(r)} \right)] \right. \right. \\ &\quad \left. \left. - (\sigma \ell)^2 P_{\nu(\bar{\kappa})}^{\ell} \left(\frac{1}{\sigma p(r)} \right) R_{\nu(\bar{\kappa})}^{\ell} \left(\frac{1}{\sigma p(r)} \right) \right. \right. \\ &\quad \left. \left. - \bar{\sigma} [\bar{\kappa}^2 \tilde{r}^2 I'_{\bar{\sigma} \ell}(\bar{\kappa} \tilde{r}) K'_{\bar{\sigma} \ell}(\bar{\kappa} \tilde{r}) + (\bar{\sigma} \ell)^2 I_{\bar{\sigma} \ell}(\bar{\kappa} \tilde{r}) K_{\bar{\sigma} \ell}(\bar{\kappa} \tilde{r})] \right\} + \left(\xi - \frac{1}{6} \right) \frac{\mathcal{R}}{4\pi} \right. \\ &\quad \left. + \frac{1}{\pi^2} \int_0^{\infty} d\lambda [\bar{\kappa}^2 \tilde{r}^2 K'_{i\lambda}(\bar{\kappa} r) K'_{i\lambda}(\bar{\kappa} \tilde{r}) + \lambda^2 K_{i\lambda}(\bar{\kappa} r) K_{i\lambda}(\bar{\kappa} \tilde{r})] \frac{\sinh \left[\frac{\lambda}{\bar{\sigma}} \pi (\bar{\sigma} - 1) \right]}{\sinh \frac{\lambda}{\bar{\sigma}} \pi} \right), \quad (46) \end{aligned}$$

where we have defined

$$R_{\nu(\bar{\kappa})}^{\ell} \left(\frac{1}{\sigma p(r)} \right) = \frac{\Gamma(\nu(\bar{\kappa}) - \ell + 1)}{\Gamma(\nu(\bar{\kappa}) + \ell + 1)} \left(\frac{C_{\bar{\kappa}, \ell}}{D_{\bar{\kappa}, \ell}} P_{\nu(\bar{\kappa})}^{\ell} \left(\frac{1}{\sigma p(r)} \right) + Q_{\nu(\bar{\kappa})}^{\ell} \left(\frac{1}{\sigma p(r)} \right) \right), \quad (47)$$

and, for $r > r_0$,

$$\begin{aligned} \left\langle \frac{1}{r^2} (\mathcal{D}_r \phi)^2 - \frac{1}{r^2} (\partial_{\theta} \phi)^2 \right\rangle &= \frac{1}{2\pi r^2} \int_{\mu}^{\infty} d\bar{\kappa} \bar{\kappa} \left(\frac{\sigma}{\pi} \sum_{\ell=0}^{\infty} B_{\bar{\kappa}, \ell} [\bar{\kappa}^2 r^2 K'_{\sigma \ell}(\bar{\kappa} r) K'_{\sigma \ell}(\bar{\kappa} r) - (\sigma \ell)^2 K_{\sigma \ell}(\bar{\kappa} r) K_{\sigma \ell}(\bar{\kappa} r)] \right. \\ &\quad \left. + \frac{1}{\pi^2} \int_0^{\infty} d\lambda [\bar{\kappa}^2 r^2 K'_{i\lambda}(\bar{\kappa} r) K'_{i\lambda}(\bar{\kappa} r) + \lambda^2 K_{i\lambda}(\bar{\kappa} r) K_{i\lambda}(\bar{\kappa} r)] \frac{\sinh \left[\frac{\lambda}{\bar{\sigma}} \pi (\sigma - 1) \right]}{\sinh \frac{\lambda}{\bar{\sigma}} \pi} \right). \quad (48) \end{aligned}$$

In all of these expressions, we have subtracted the point string contribution and then added it back via the integral representation in Eq. (35). The counterterm proportional to \mathcal{R} in Eq. (46) represents a scaling factor, similar to the logarithmic term described above, corresponding to our choice of $\bar{\sigma}$ and \tilde{r} for the point string subtraction. As a check of this calculation, we find numerically that these results obey the conservation law in Eq. (44).

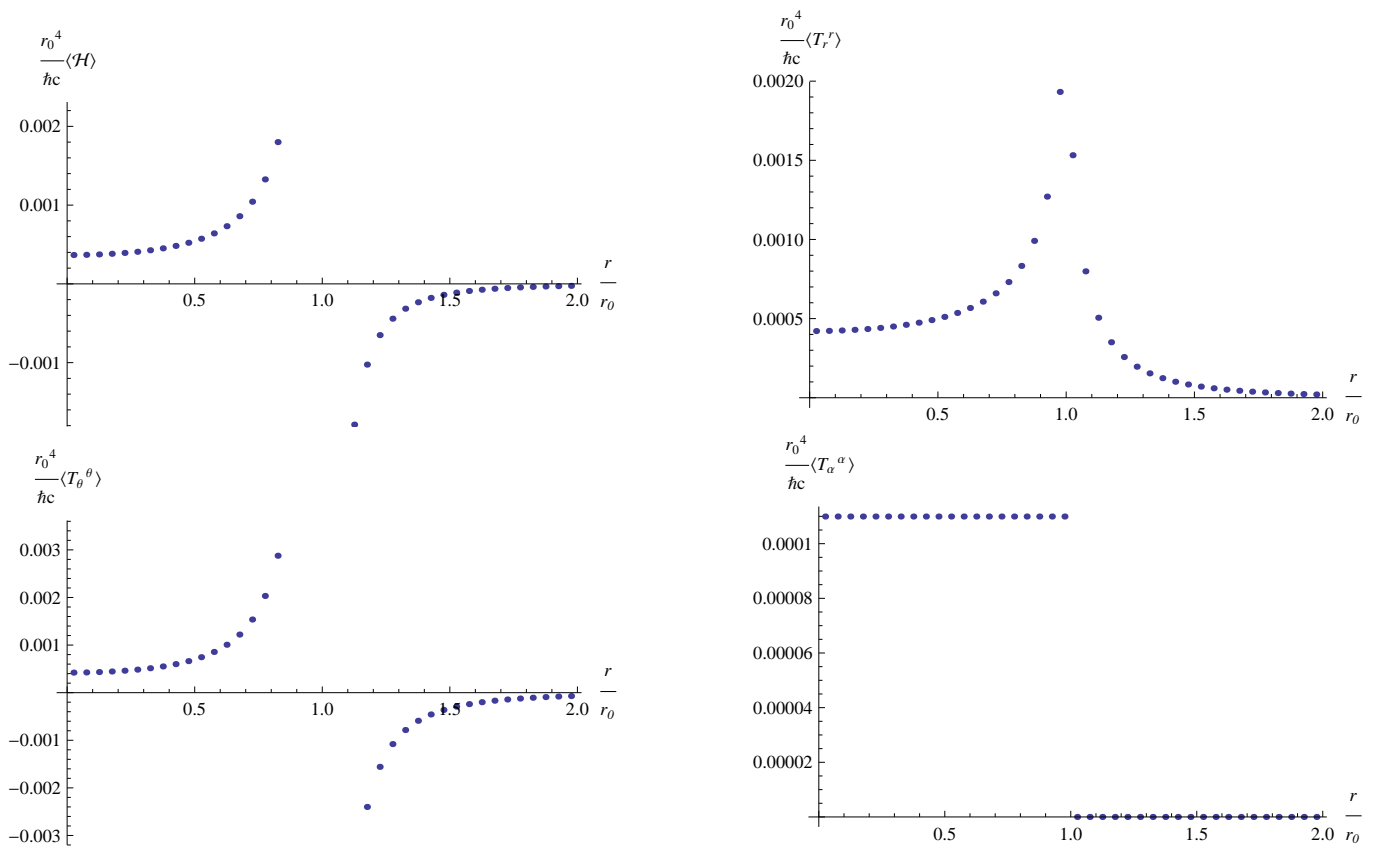


FIG. 1: Renormalized energy density $\langle \mathcal{H} \rangle$, top left, radial pressure $\langle T_r^r \rangle$, top right, angular pressure $\langle T_\theta^\theta \rangle$, bottom left, and stress-energy tensor trace $\langle T_\alpha^\alpha \rangle$, bottom right, in units of $\frac{\hbar c}{r_0^4}$, as functions of r , in units of r_0 , for deficit angle $\theta_0 = \frac{\pi}{3}$, field mass $\mu = 0$, renormalization scale $M = \frac{i}{r_0}$, and conformal coupling $\xi = \frac{1}{6}$. The stress-energy tensor trace arises entirely from the anomaly contribution, Eq. (32).

VII. RESULTS

We can now compute renormalized expectation values numerically by summing over ℓ and integrating over $\bar{\kappa}$. Figures 1 and 2 show the components of the stress-energy tensor and its trace, for a massless field renormalized at the scale of the string radius, $M = \frac{i}{r_0}$, in the case of conformal and minimal coupling respectively. For conformal coupling, the trace is given entirely by the anomaly contribution, Eq. (32). Consistent with the result from the point string, the radial pressure is always positive, while the other components switch sign both inside and outside the string and between conformal and minimal coupling. The singularity at $r = r_0$ is an artifact of the discontinuity in the curvature, which in an actual string would decrease to zero continuously. The integrals of these quantities over space, taken as principal values, remain finite [12], although they are difficult to compute numerically because of this behavior.

Another quantity of interest is the contribution to the null energy condition (NEC). Energy conditions represent restrictions on the stress-energy tensor that can potentially rule out exotic phenomena, such as closed timelike curves or superluminal travel. The null energy condition, $T_{\alpha\beta}u^\alpha u^\beta \geq 0$ for a null 4-velocity u^α has known violations, but the weaker condition in which it is averaged over an achronal null geodesic (AANEC) may still be viable, and is sufficient to rule out exotic phenomena [21, 22]; while examples that violate this condition in have been found [23, 24], they are expected only to exist for quantum fields in curved spacetime [13, 13, 25–28], and it is not known whether such violations can be self-consistently constructed from solutions to the Einstein equation.

Here we consider the contribution from quantum fluctuations, to which we would then add the classical contribution of the matter that is creating the string. By Einstein's equation for the classical string background as given in Eq. (6),

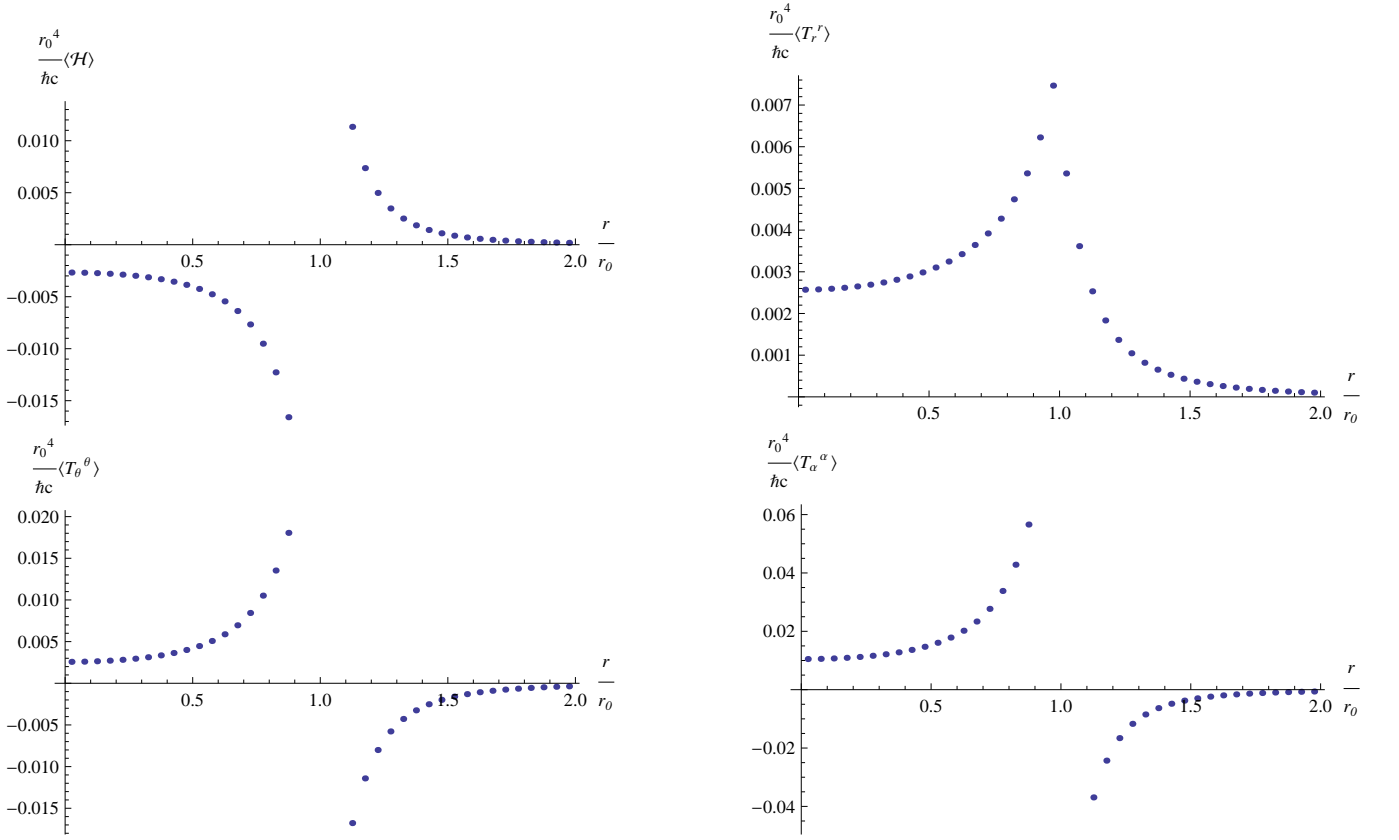


FIG. 2: Renormalized energy density $\langle \mathcal{H} \rangle$, top left, radial pressure $\langle T_r^r \rangle$, top right, angular pressure $\langle T_\theta^\theta \rangle$, bottom left, and stress-energy tensor trace $\langle T_\alpha^\alpha \rangle$, bottom right, in units of $\frac{\hbar c}{r_0^4}$, as functions of r , in units of r_0 , for $\theta_0 = \frac{\pi}{3}$, field mass $\mu = 0$, renormalization scale $M = \frac{i}{r_0}$, and minimal coupling $\xi = 0$.

the latter has $T_{tt} = -T_{zz} = \frac{\mathcal{R}}{16\pi G} > 0$, with other components zero [6], and therefore gives a contribution that should only reduce the possibility that AANEC is violated. We consider a radial geodesic with 4-velocity $u^\alpha = \left(1 \frac{1}{p(r)} 0 0\right)$, which obeys the geodesic equation $u^\alpha \nabla_\alpha u^\beta = 0$. The integrand of the AANEC integral

$$\int_0^\infty dr p(r) \langle T_{\alpha\beta} u^\alpha u^\beta \rangle = \int_0^\infty dr p(r) \langle \mathcal{H} + T_r^r \rangle \quad (49)$$

is shown in Fig. 3 for both minimal and conformal coupling. For minimal coupling, the integral over the geodesic is difficult to determine because it appears to be close to zero, with the singularity at $r = r_0$ preventing a detailed calculation, while for conformal coupling the integral appears to be positive, indicating that the condition is obeyed by the quantum contribution.

VIII. CONCLUSIONS

We have demonstrated a complete calculation of the renormalized quantum stress-energy tensor in the background of a “ballpoint pen” cosmic string geometry in $3 + 1$ dimensions. This example represents one of the few cases in which quantum effects in curved spacetime can be calculated in detail, and concretely demonstrates the role played by the conformal trace anomaly in the renormalization process, for both the full four-dimensional spacetime in which the calculation is carried out and the two-dimensional subspace in which it has nontrivial curvature. This result also allows one to calculate the quantum field’s contribution to the averaged null energy condition, which appears to be obeyed.

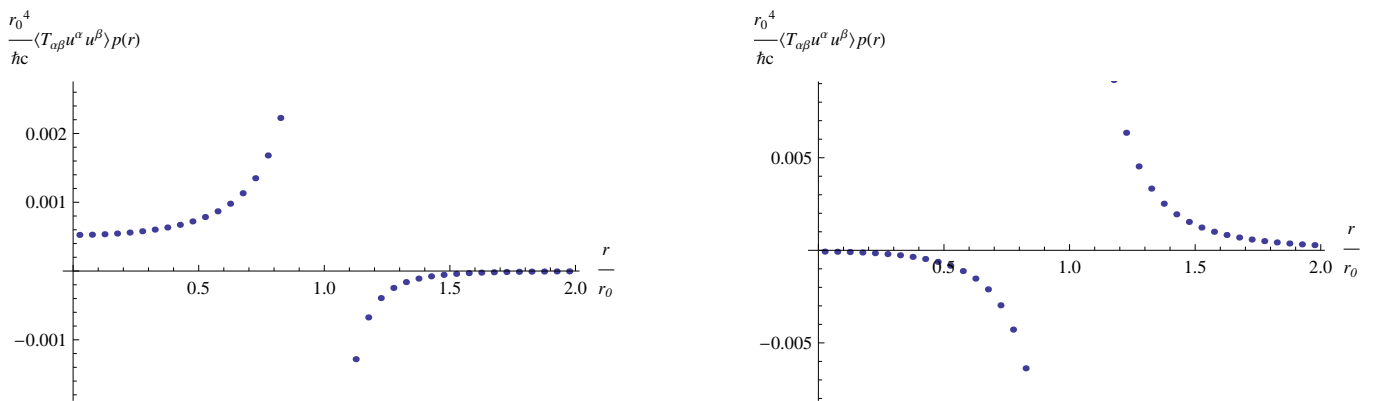


FIG. 3: Contribution to the averaged null energy condition integral for a radial geodesic, $\langle T_{\alpha\beta} u^\alpha u^\beta \rangle p(r) = \langle \mathcal{H} + T_r^r \rangle p(r)$, in units of $\frac{\hbar c}{r_0^4}$, as a function of r , in units of r_0 , for $\theta_0 = \frac{\pi}{3}$, field mass $\mu = 0$, renormalization scale $M = \frac{i}{r_0}$. The left panel shows conformal coupling $\xi = \frac{1}{6}$, while the right panel shows minimal coupling $\xi = 0$.

While these calculations have been carried out in three space dimensions, it is straightforward to reduce to the previously considered case of two space dimensions [8]: in computing the expectation values we divide by $\sqrt{\bar{\kappa}^2 - \mu^2}$ in all of the $\bar{\kappa}$ integrands, the $\langle (\partial_t \phi)^2 \rangle$ integral is multiplied by 4 while the other integrals are multiplied by 2, [12] and all k_z , $\partial_z \phi$, second-order counterterm, and anomaly contributions are set to zero. It is also straightforward to extend these calculations to the “flowerpot” model, in which the curvature is entirely concentrated in a δ -function contribution at $r = r_0$, simply by making the appropriate substitution of scattering wavefunctions [7, 8]. In that case, however, the curvature is always zero for $r \neq r_0$, so all counterterms and anomaly contributions vanish, and we cannot analyze the AANEC for a radial geodesic because it must pass through the singularity at $r = r_0$. One could also consider a curvature background that goes to zero continuously for increasing r , rather than as a step or δ -function. In this case, the scattering wavefunctions would likely need to be computed numerically, for example by using variable phase techniques [29], and there would be additional contributions to the second-order counterterm and corresponding anomaly contribution proportional to $\square \mathcal{R}$.

It would also be interesting to calculate the integrals over space of these local densities. In flat spacetime, these calculations can be implemented effectively by making use of the relationship between the integral over space of the difference between the free and interacting Green’s functions and the Jost function $F_\ell(\bar{\kappa})$ in scattering channel ℓ [29],

$$2\bar{\kappa} \int_0^\infty dr \left[G_\ell(r, r, \bar{\kappa}) - G_\ell^{(0)}(r, r, \bar{\kappa}) \right] = \frac{d}{d\bar{\kappa}} \log F_\ell(\bar{\kappa}), \quad (50)$$

and both exact and approximate expressions for the ballpoint pen Jost function have been obtained in Refs. [16, 17]. A similar approach here would need to take into account the different topology between the full and free backgrounds. Such an approach can potentially avoid the difficulties associated with integrating over the singularity at $r = r_0$ and provide generally applicable insights into whether the AANEC is obeyed.

IX. ACKNOWLEDGMENTS

It is a pleasure to thank K. Olum for sharing preliminary work on this topic and M. Koike, X. Laquidain, and H. Weigel for helpful conversations and feedback. N. G. was supported in part by the National Science Foundation (NSF) through grant PHY-2205708.

-
- [1] N. D. Birrell and P. C. W. Davies, *Quantum Fields in Curved Space*, Cambridge Monographs on Mathematical Physics (Cambridge University Press, Cambridge, 1982).
[2] T. M. Helliwell and D. A. Konkowski, Phys. Rev. D **34**, 1918 (1986).
[3] B. Linet, Phys. Rev. D **35**, 536 (1987).
[4] V. P. Frolov and E. M. Serebriany, Phys. Rev. D **35**, 3779 (1987).

- [5] W. A. Hiscock, *Phys. Rev. D* **31**, 3288 (1985).
- [6] I. Gott, J. R., *Astrophys. J.* **288**, 422 (1985).
- [7] B. Allen and A. C. Ottewill, *Phys. Rev. D* **42**, 2669 (1990).
- [8] M. Koike, X. Laquidain, and N. Graham, *Phys. Rev. D* **110**, 105009 (2024).
- [9] P. C. W. Davies, S. A. Fulling, and W. G. Unruh, *Phys. Rev. D* **13**, 2720 (1976).
- [10] P. C. W. Davies and S. A. Fulling, *Proceedings of the Royal Society of London Series A* **354**, 59 (1977).
- [11] S. M. Christensen and S. A. Fulling, *Phys. Rev. D* **15**, 2088 (1977).
- [12] K. D. Olum and N. Graham, *Physics Letters B* **554**, 175 (2003).
- [13] E. E. Flanagan and R. M. Wald, *Phys. Rev. D* **54**, 6233 (1996).
- [14] D. Schwartz-Perlov and K. D. Olum, *Phys. Rev. D* **72**, 065013 (2005).
- [15] J. R. Fliss, B. Freivogel, E.-A. Kontou, and D. P. Santos, *SciPost Phys.* **16**, 119 (2024).
- [16] N. R. Khusnutdinov and M. Bordag, *Phys. Rev. D* **59**, 064017 (1999).
- [17] N. R. Khusnutdinov and A. R. Khabibullin, *Gen. Rel. Grav.* **36**, 1613 (2004).
- [18] N. Graham and H. Weigel, *Physics Letters B* **852**, 138638 (2024).
- [19] D. Deutsch and P. Candelas, *Phys. Rev. D* **20**, 3063 (1979).
- [20] I. Brevik and M. Lygren, *Annals of Physics* **251**, 157 (1996).
- [21] N. Graham and K. D. Olum, *Phys. Rev. D* **76**, 064001 (2007).
- [22] A. C. Wall, *Phys. Rev. D* **81**, 024038 (2010).
- [23] D. Urban and K. D. Olum, *Phys. Rev. D* **81**, 024039 (2010).
- [24] E.-A. Kontou and K. Sanders, *Classical and Quantum Gravity* **37**, 193001 (2020).
- [25] R. Bousso, Z. Fisher, J. Koeller, S. Leichenauer, and A. C. Wall, *Phys. Rev. D* **93**, 024017 (2016).
- [26] T. Hartman, S. Kundu, and A. Tajdini, *JHEP* **07**, 066 (2017).
- [27] E.-A. Kontou and K. D. Olum, *Phys. Rev. D* **87**, 064009 (2013).
- [28] E.-A. Kontou and K. D. Olum, *Phys. Rev. D* **92**, 124009 (2015).
- [29] N. Graham, R. Jaffe, V. Khemani, M. Quandt, M. Scandurra, and H. Weigel, *Nucl. Phys. B* **645**, 49 (2002).